Scientific Report 2013-2014

Ideas program. Exploratory research projects

Implementation of project Cod PN-II-ID-2012-4-0028:
Alkali and silver halides based magnetic tunnel junctions
September 2013- December 2014

Report: September.02.2013-December.31.2013

Objectives:

1. Structural, electronic, magnetic and spin dependent transport properties of Fe/CaS/Fe (001) heterostructures.

2. Impact of Fe/NaCl (001) interface structure on physical properties of Fe/NaCl/Fe (001) heterojunctions.

3. Magnetic properties of the half-metallic systems of B_1-type.

The objectives included in the 2013 year research program have been realized as evidenced in the following report.

1. Structural, electronic, magnetic and spin dependent transport properties of Fe/CaS/Fe (001) heterostructures.

1.1 Electronic structure of CaS compound

The band structure of CaS has been determined by using TB-LMTO formalism, in the atomic sphere approximation (ASA) and the exchange correlation potential expressed within Vosko-Wilk-Nussair parameterization. The CaS is an indirect band gap semiconductor having the top of the valence band at the Γ_{15} point and the bottom of the conduction band at X_3 point, respectively – Fig.1.1. The band gap is of 0.146 Ry. The lower part of the valence bands corresponds to S(3s) states and it is separated by the upper valence bands by a gap of ≅ 0.5 Ry. The upper valence bands correspond predominantly to S(3p) states with some small contributions from 4s, 4p and 3d states of calcium. The conduction band consists predominantly from Co(3d) and Ca(4s) states, respectively.

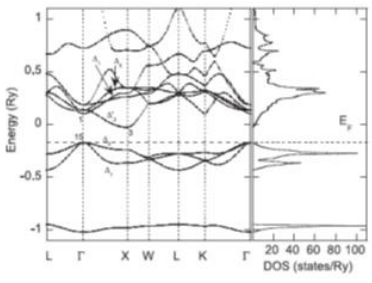


Fig.1.1

1.2 Magnetic properties of Fe/CaS/Fe (001) tunnel junctions

Admitting a 6Fe/9CaS/7Fe heterostructure, the magnetic properties were computed considering two possible configurations: (a) with Fe atoms sitting above Ca and S sites (IC_1) and (b) with iron atoms located above the hollow sites between Ca and S ions (IC_2). Starting from the above configurations, the charge transfers and magnetic profiles of the above heterostructures were determined – Fig.1.2. For both IC_1 and the IC_2 interface configurations the charge transfer is relatively small and mostly localized at interfaces. In case of IC_1 interface configuration, due to higher electronegativity of sulphur, the charge depletion is slightly higher for Fe_2 atoms sitting above anionic S positions. As a consequence of different charge transfer for interfacial iron atoms, at the Fe/CaS (001) interfaces with IC_1 configuration, there is a charge density which oscillate in antiphase, with the charge distribution in the interfacial CaS layer, resulting in a reduction of the electrostatic energy interaction and enhancing the interface stability. The enhancement of the iron interfacial magnetic moment is higher at the IC_1 geometry (2.92 μ_B) as compared with that at IC_2 configuration (2.46 μ_B).

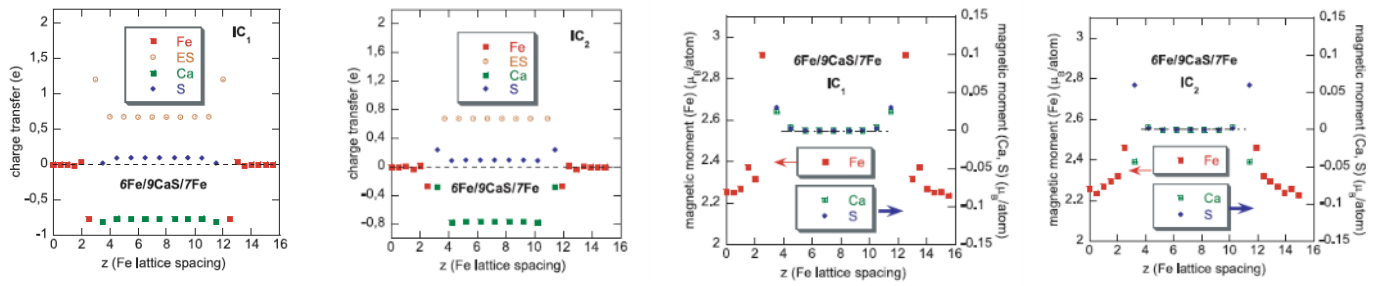


Fig.1.2

1.3 Transport properties of tunnel junctions

The evolution of spin dependent conductivities and of TMR ratio with barriers thicknesses, for 6Fe/mCaS/7Fe(001) tunnel junctions are presented in Fig.1.3. For both interface configurations all conductances decay exponentially with the barrier width. In case of IC_1 interface configuration, the minority spin FM conductance is slightly higher than the others and TMR reaches a maximum (350 %) for 7-8 MLs. For heterostructures with IC_2 interface, the minority spin FM conductance has the lowest decay rate, compared with the majority spin FM and both AFM conductances and TMR reaches a maximum (5000 %) for 10 MLs.

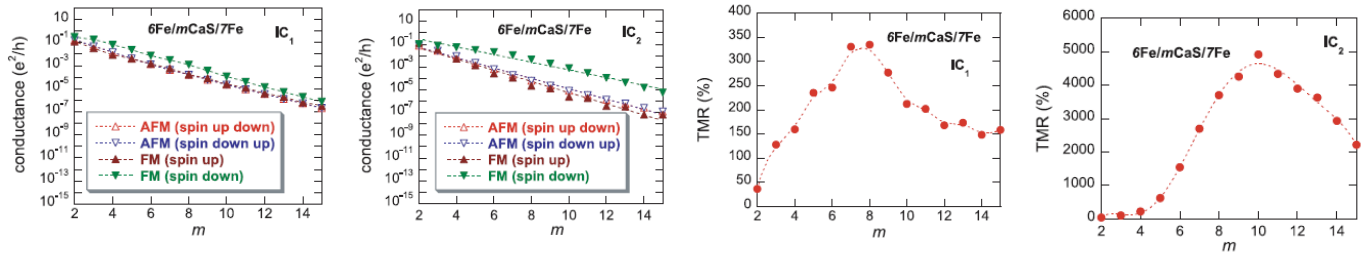


Fig.1.3

The $k_{\|}$ resolved partial conductances of 6Fe/mCaS/7Fe(001) tunnel junctions with m = 5 and 9, for both IC_1 and IC_2 interfaces structures, were determined. Some results are given in Fig.1.4. The tunneling currents change considerably with the spin channel and depend also on the Fe/CaS (001) interface structure. The main contributions to the FM conductance, for heterostructures with IC_1 interface configuration are given by Δ_1 states, which present a broad peak around Γ point, as well as the Δ_5 states. In the case of IC_2 interface configuration, Δ_1 states centered at Γ point are decoupled by the interface structure. The Δ_1 states have s, p_z and d_{z^2} wave function symmetry. At IC_1 interfaces, due to strong $Fe(3d_{z^2}) - S(3p_z)$ hybridization, Δ_1 states will have an important contribution to the majority spin FM conductance, while at IC_2 interfaces, breaking Fe-S bonding, will result in a decrease of Δ_1 states contribution to the majority spin FM conductance.

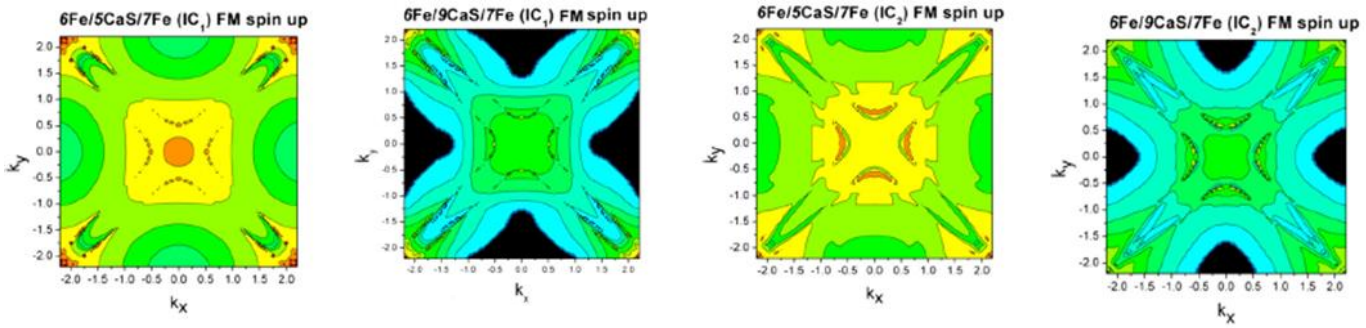


Fig.1.4

As a conclusion, can be evidenced that a TMR value of 5000 % can be theoretically obtained in a Fe/CaS/Fe(001) junctions for a IC_2-type interface.

The scientific results were published in the paper

"Structural, electronic, magnetic and spin dependent transport properties of Fe/CaS/Fe(001) heterostructures" **P. Vlaic, E.Burzo,** K. Carva, J. Appl.Phys. 113, 053715 (2013) – „hot paper" IF=2.185

2. Impact of Fe/NaCl (001) interface structure on physical properties of Fe/NaCl/Fe(001) heterojunctions.

2.1 The Fe/NaCl/Fe (001) interface stability in in c(2x2) superstructure

Due to small misfit between Fe and NaCl lattices, at Fe/NaCl(001) interfaces, the stability of the system considering three types of interfaces (IC_1, IC_2, IC_3) has been analysed – Fig.2.1, 2.2 and 2.3. Self-consistent energy calculations for both FM and AFM states of magnetic electrodes, yield an equilibrium lattice constant of a ≅ 2.75 Å, independent on the interface geometry. The above value is little smaller than either the experimental lattice spacing of Fe or half of experimental lattice constant of NaCl. The LSDA formalism, generally underestimate the lattice spacing by a few percents. The Fe/NaCl/Fe(001) heterostructures with IC_1, Fe/NaCl(001) interfaces, have lower total energies compared to those having

IC_2 interfacial configuration, for a < 2.95 Å – Fig.2.3. Thus, IC_1 interface configuration seems to be optimal, both for equilibrium lattice constants or those experimentally determined.

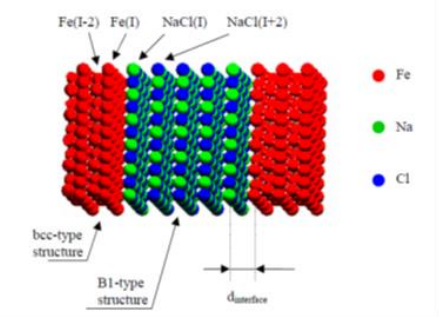


Fig.2.1

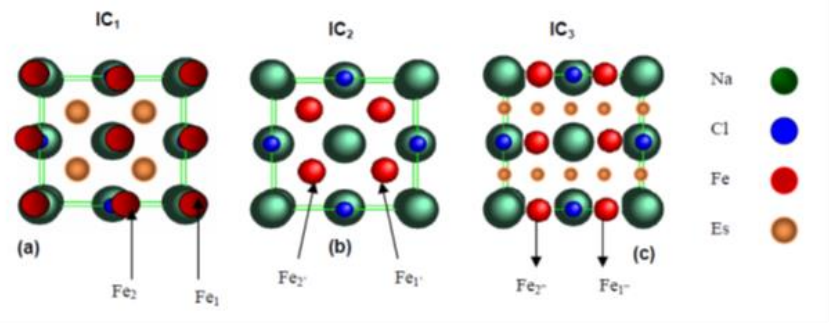


Fig.2.2

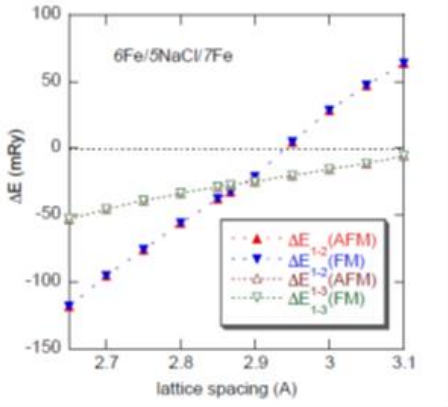
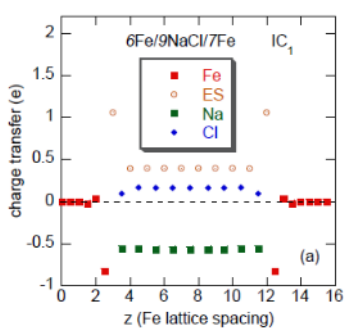


Fig.2.3

2.2 Ground state magnetic properties in correlation with interfacial structure

The layer- and atom-decomposed spin-polarized DOS have been studied for 6Fe/9NaCl/Fe(001) heterostructures with IC_1, IC_2 and IC_3 interface configurations. The data obtained for IC_1-type are given in Fig.2.4. The charge transfer is small and mostly localized at Fe/NaCl(001) interface. Consistently with higher electronegativity of chlorine, the charge diminution is higher for interfacial Fe_2(I) atoms sitting above anionic IC_1 positions than for Fe_1(I) ones located atop to cationic Na sites. As a result, the density of charge in the interfacial Fe layers fluctuates in antiphase with the charge of interfacial Na and Cl ions, minimizing the electrostatic energy interaction and enhancing the Fe/NaCl(001) interface stability. The interlayer exchange coupling in Fe/NaCl/Fe(001) heterostructures is small FM, for IC_1 and IC_3 interfacial geometries, whereby for IC_2 interfacial configuration is AFM. For all studied heterojunctions the exchange couplings decrease exponentially with the barrier thicknesses. For heterojunctions with IC_1 interfacial geometry, the minority-spin FM conductance is largest, particularly for thicker barriers. The spin polarization of FM tunneling current rapidly increases and values of $3.2 \cdot 10^4$ % were computed for 6Fe/mNaCl/7Fe junctions having m > 10 – Fig.2.5. For IC_2 and IC_3 configurations the TMR values are little dependent on the barrier width and are below 500 %.



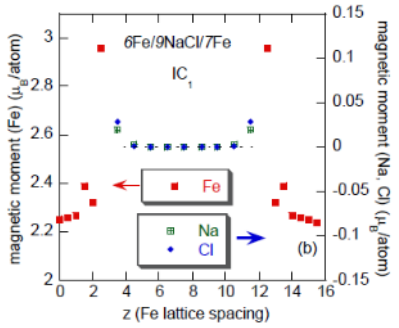


Fig.2.4

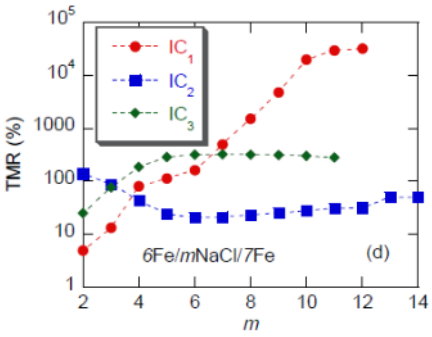


Fig.2.5

The effect of interdiffusion on the electronic and spin polarized transport properties of Fe/NaCl/Fe (001) heterostructures has been analysed for the most stable IC_1, Fe/NaCl(001) interfacial configuration – Fig.2.6. The Na interdiffusion described by $Fe_2(Fe_1)_{1-x}Na_x/Na_{1-x}Fe_xCl$ as well as the Cl interdiffusion $Fe_1(Fe_2)_{1-x}Cl_x/NaCl_{1-x}Fe_x$ are not favorable, but the disorder at interfaces may strongly affect the electronic transport properties. Absence of interfacial interdiffusion together with the small lattice mismatch between Fe and NaCl layers are important advantages of Fe/NaCl/Fe (001) junctions for the purpose of spintronic applications.

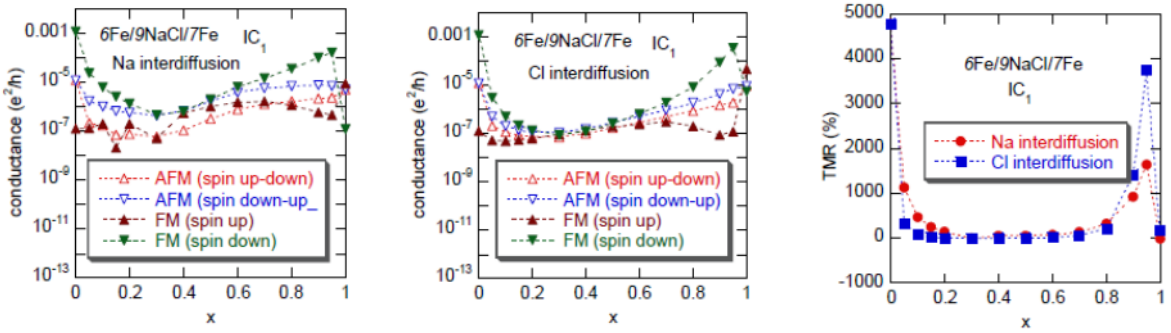


Fig.2.6

The scientific results on this system were published in the paper

"Impact of Fe/NaCl(001) interface structure on electronic, magnetic and spin-polarized transport properties Fe/NaCl/Fe(001) heterojunctions: an ab initio study", **P. Vlaic, E.Burzo** and K.Carva, Journal of Alloys and Compounds, 598, 41-53 (2014) IF = 2.734.

3. Magnetic properties of B_1 half-metallic systems

3.1 Magnetic properties of bulk materials

The half-metallic materials have a metallic behavior for one spin direction and consequently, the spin polarization at Fermi level is 100 %. The metastable, half metallic SrC compound, has been studied. The equilibrium lattice parameter is a = 5.55 Å and a magnetic moment per formula unit M = 2 μ_B has been determined. Thus, this compound is epitaxial compatible with NaCl-type barrier (a = 2.64 Å) which has a B_1 band direct gap as well as with CaS (a= 5.96 Å) having a Γ-X indirect gap.

3.2 Physical properties of junctions

The ground state magnetic and electronic properties, of the SrC/NaCl(CaS)/SrC(001) multilayers structure were studied – Fig.3.1. In this system the epitaxial relations between the layers are of SrC[100]||[100]NaCl(CaS); Pd[110]||SrC[100].

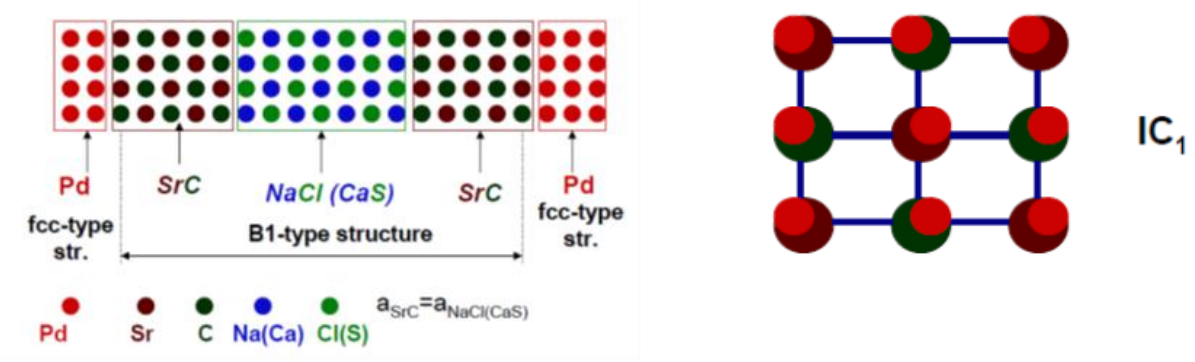


Fig.3.1

The magnetic and electronic properties of 2Pd/5SrC/9NaCl/5SrC/3Pd(001) are given in Fig.3.2. There is a small interface charge transfer at SrC/NaCl(CaS)(001) interfaces. As a result, the Sr and C magnetic moments are only little diminished as compared to those of bulk sample. The spin polarizations, induced on Cl(S) and Na(Ca) interfacial positions, are relative small.

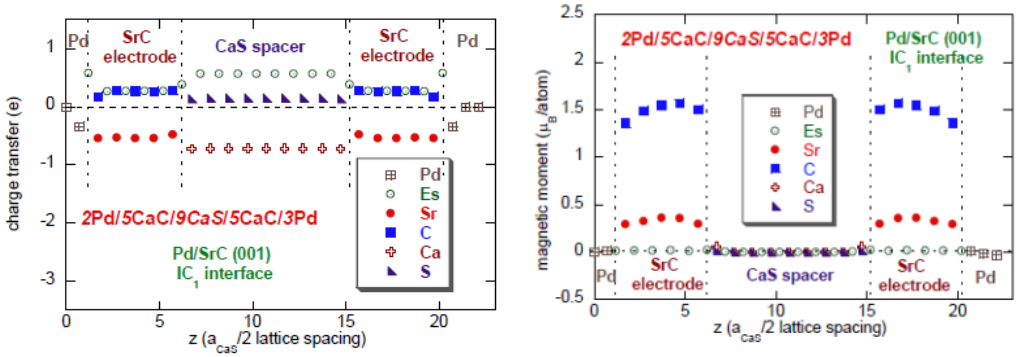
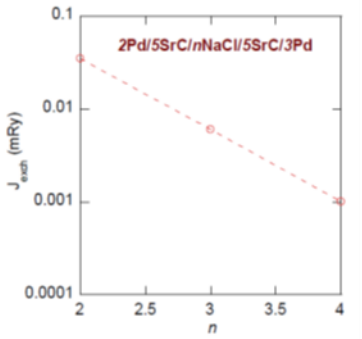


Fig.3.2

The exchange coupling in the NaCl-based junctions is ferromagnetic, while for the case of CaS is antiferromagnetic. There are small couplings for both SrC/NaCl/SrCl(001) and SrC/CaS/SrC(001) superstructures, which decay exponentially with barrier width. The same behavior can be seen in Fig.3.3, for 2Pd/5SrC/nNaCl/CaS/5SrC/3Pd multilayer configuration.



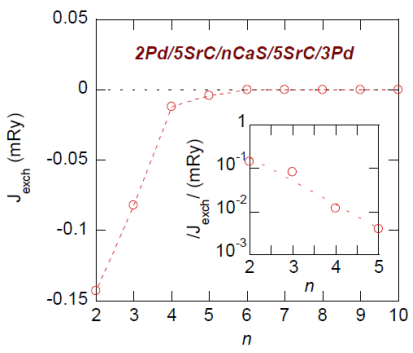


Fig.3.3

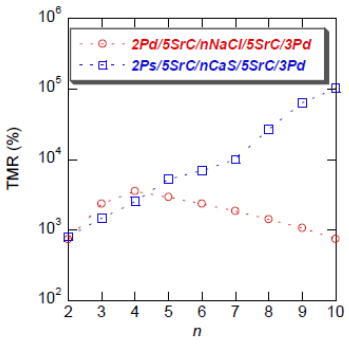


Fig.3.4

The magnetoresistivity of magnetic tunnel junctions, based on CaS, exponentially increases with the barrier width – Fig.3.4. When using NaCl barrier, the tunneling magnetoresistivities have a maximum value of $4 \cdot 10^3$ % for n = 4 layers.

The scientific results on this system were presented at"Fifth Seeheim Conference on Magnetism" Frankfurt, Germany, 29.09 – 3.10.2013, ***"Magnetic and spin dependent transport properties of SrC/NaCl/(CaS)/SrC (001) tunnel junctions"*** by **P. Vlaic, E. Burzo**

In the framework of the project we studied also the pressure effects of the magnetic properties of RCo_5 (R = Y, Gd) compounds, having possible technical applications. Isomorphic transitions were evidenced for relatives volumes $v/v_0 = 0.91$ and 0.86 for YCo_5 and $GdCo_5$, respectively. The magnetic to non-magnetic transition is a two-step process.

The results were published in the paper:

"Pressure effects on crystal structures and magnetic properties of RCo_5 (R = Y or Gd) compounds" **E.Burzo, P. Vlaic**, AIP Conf. Proc. 1564, 96 (2013).

2014 Year Report

Objectives:

1. Magnetic tunnel junction of Fe/AgCl/Fe (001)

2. Physical properties of tunnel junctions of CaC/X/CaC(001) with X = LiCl

The above objectives, included in working plane for 2014 year, has been realized. In addition, the theme 3 of the research program for 2015 has been also partially finalized. Thus, physical properties of the $(Ca,La,Fe,Mo)O_6$-based double perovskites were also studied. The scientific results on this matter are now published in J. Alloys and Compounds (2015). During the 2014 year, at International Conferences were also presented three invited lectures, one oral presentation and one poster paper, included in this report.

1. Fe/AgCl/Fe (001) magnetic tunnel junctions

The Fe/AgCl/Fe(001) junction structure involves the presence of iron electrodes having cvc-type structure and a B_1-type structure for AgCl. For the Fe/AgCl(001) interface an epitaxial relation Fe(001)[100]||[100]AgCl[001] has been considered. Two model interfaces were analysed, denoted as IC_1 (Fe atoms sitting atop Ag and Cl positions) and IC_2 (Fe atoms located above the hollow sites between Ag and Cl ions), respectively. Self-consistent calculations show that both Fe/AgCl/Fe(100) heterostructures are stable, as illustrated in case of 6Fe/5AgCl/7Fe (001) configuration – Fig.1.1. An equilibrium lattice

spacing of ≅ 2.75 Å, independent on the interfacial configuration and magnetic state, has been determined. The above value is by 4 % smaller than that of bulk iron.

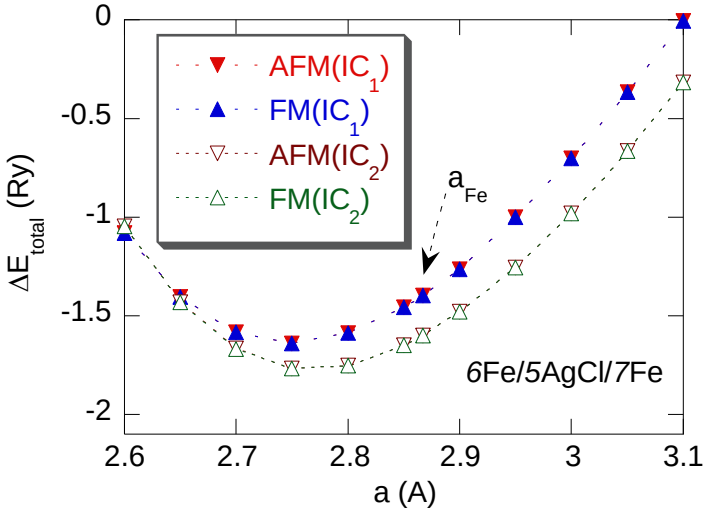


Fig.1.1

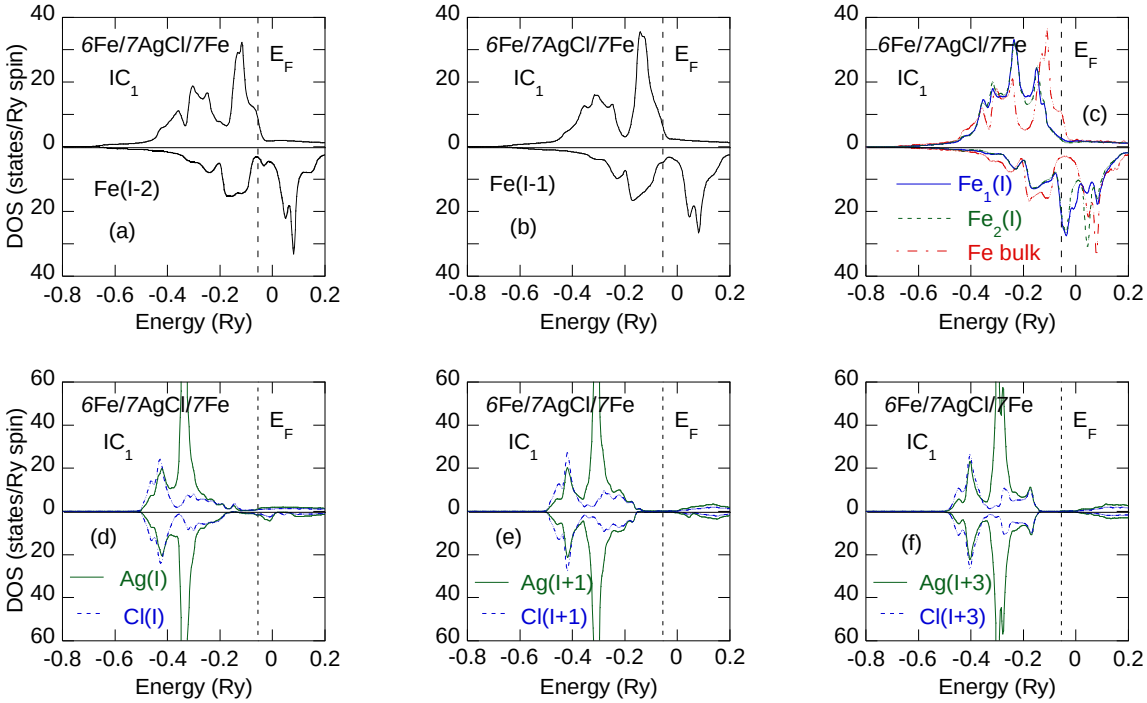


Fig.1.2

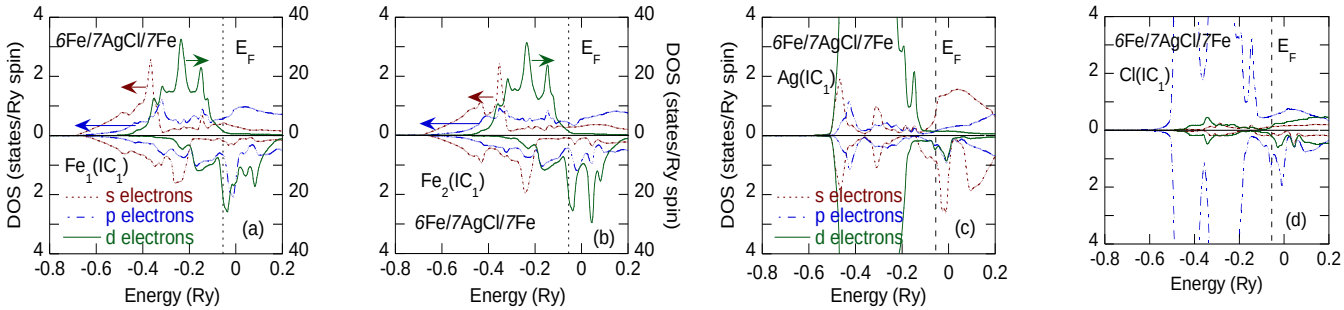


Fig.1.3

The layer and atom-resolved spin-polarized density of states (DOS) of 6Fe/5AgCl/7Fe(001) heterostructure with IC_1, Fe/AgCl(001) model interface, are given in Fig.1.2, while in Fig.1.3 are plotted the l-resolved DOS of interfacial Fe, Ag and Cl atoms in IC_1 configuration. As result of interactions between Fe and AgCl interfacial layers, iron induced gap states (MIGS) are observed in AgCl barriers, near interfaces – Fig.1.2d. The induced states appear on both Al and Cl ions making Fe/AgCl (001) interfaces practically metallic.

Layer-decomposed charge transfer, relative to valence charge of neutral atom, as well as the magnetization profiles of 6Fe/7AgCl/7Fe(001) heterostructures with IC_1 and IC_2 interfacial geometries are shown in Fig.1.4. Since the Fermi level of iron is located near the bottom of the AgCl conduction band, a charge transfer will occurs. As a result, MIGS in the band gap of the barrier are formed.

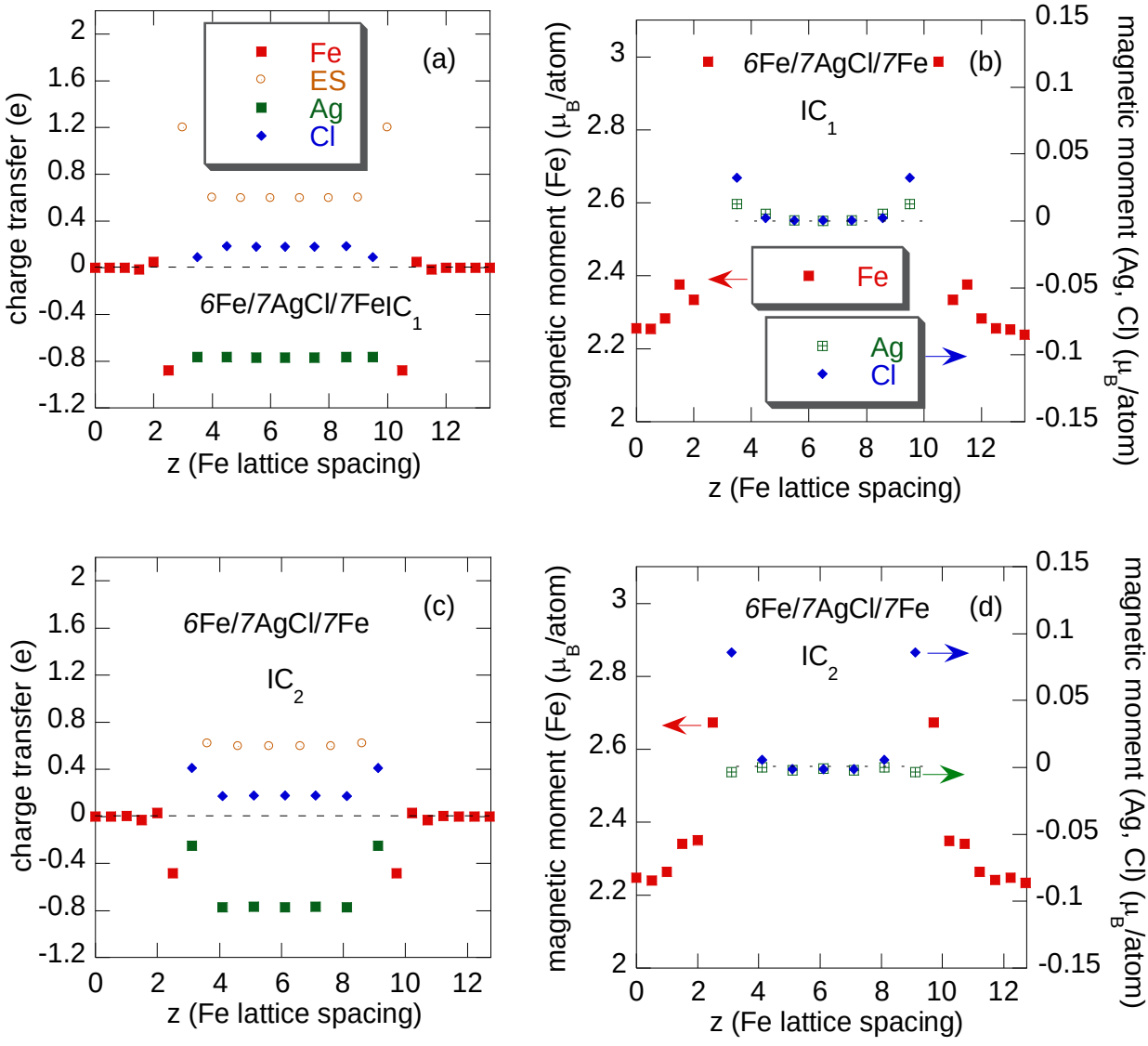


Fig.1.4

The iron magnetic moment, at IC_1 surface, is enhanced as compared to their bulk value. A smaller increase of the iron moments can be shown for IC_2 configuration. In this case, there is a higher degree of Fe3d band hybridization.

For both heterostructures (IC_1, IC_2), the exchange coupling oscillates along the interlayer between FM and AFM states, having an evolution quite specific for metallic spacers – Fig.1.5. Two regimes of oscillations can be seen for both superstructures. The first one is characteristic for barriers having m = 3 for IC_1 and m = 5 for IC_2 superstructures. For thicker barriers, the exchange couplings show damped oscillations.

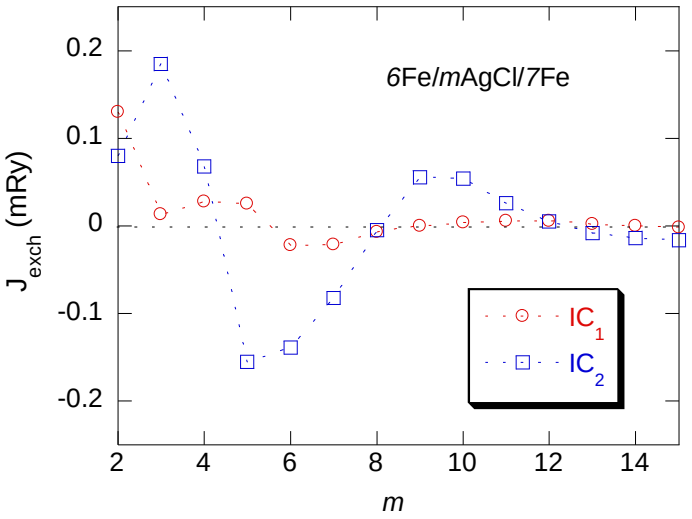


Fig.1.5

The transport properties of heterojunctions were studied. The spin resolved conductances and TMR ratio of 6Fe/mAgCl/7Fe(001) heterojunctions are given in Fig.1.6. The largest contributions to the FM conductances are due to majority-spin electrons for both IC_1 and IC_2 interfacial configurations. The majority spin FM conductances, in the asymptotic region, are less sensitive to the interface structure, while the minority-spin FM and AFM conductances depend on interfaces, particularly the IC_2 one. The higher tunneling magnetoresistance can be evidenced for IC_1 configuration. The TMR values increase with barrier width having a change in slope at m = 6. For m = 15, TMR values above 3100 % can be shown. In case of IC_2 interfacial configuration, long range oscillations, around 150 %, are evidenced.

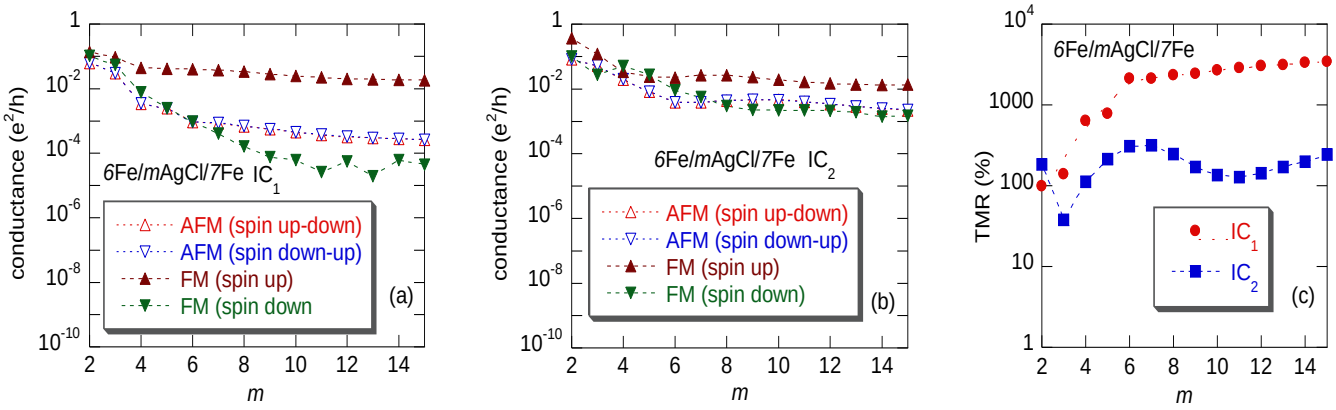


Fig.1.6

Transmission across a planar junction is determined by the barrier band structure. For both heterostructures, in the asymptotic region, majority spin FM conductances decrease exponentially confirming the tunneling across the AgCl barrier. The minority-spin FM and AFM conductances decrease too, their decay parameters being interface sensitive.

A powerful Δ_1 spin filter effect was evidenced across the AgCl barrier. The direct Γ-Γ band gap as well as the location of E_F closer to the minimum in the conduction band implies a lower Δ_1 decay parameter compared with those evidenced for MgO or NaCl barriers.

The minority-spin FM and AFM conductances are dominated by hot-spots or spike-like peaks located at $\bar{\Gamma}$ point. These spikes originate from the minority-spin interface resonant states and increase the transmission by resonant tunneling.

The interdiffusion of Ag and Cl, at Fe/AgCl(001) interfaces, considering both IC_1 and IC_2 configurations, was analysed. The Cl interdiffusion for both interfaces is not energetically favored. The Ag interdiffusion can appear at both IC_1 and IC_2 interfaces. No magnetic dead layers have been evidenced, as result of both Ag and Cl interdiffusion. The interfacial diffusion influence the junction magnetoresistive properties, particularly those having IC_1-type interface.

Small lattice mismatch between Fe and AgCl structures and the strong Δ_1 spin filter effect, across AgCl barrier, make Fe/AgCl(001) heterointerfaces of interest for spintronic applications. Their use implies the control of interfacial interdiffusion and the stabilization of flat Fe/AgCl(001) interfaces. The substitution of Ag for Na at Fe/NaCl(001) interfaces may give also the opportunity to tune the spin polarized transport across Fe/(Ag,Na)Cl/Fe(001) junctions between the resonant and direct tunneling mechanisms.

The above scientific results will appear in the paper:

"Oscillatory exchange coupling and strong direct tunneling in AgCl based heterojunctions,, **P.Vlaic, E.Burzo,** K.Carva, Journal of Alloys and Compounds, 2015 (accepted for publication).

2. Physical properties of tunnel junctions of CaC/X/CaC(001) with X = LiCl, MgS

The electronic structure of presumed CaC compound has been analysed. The dependences of the total energy on lattice parameters are given in Fig.2.1, for two structure types, namely B1 and B3, respectively. The ground state, having minimum energy, is obtained for B1 type one. The equilibrium lattice parameter is 5.20 Å. The CaC compound is near half-metallic, the spin magnetic moment, being 1.82 μ_B/f.u.

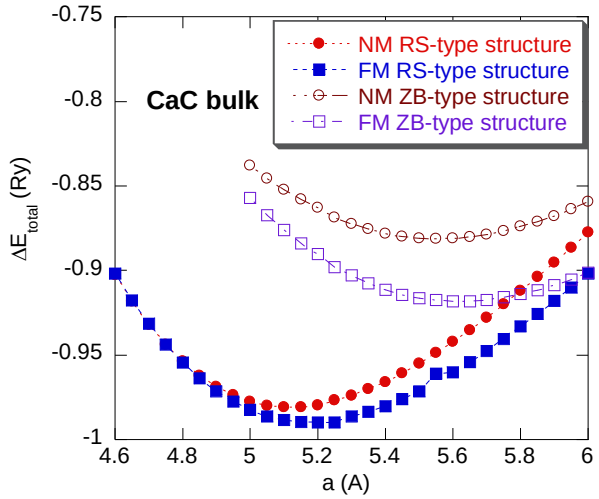


Fig.2.1

The electronic properties of CaC/LiCl/CaC(001) and CaC/MgS/CaC(001) heterostructures were studied. Their configurations are /(semi-infinit)Ca(001))/2Cu(001)/nCaC(001)/mLiCl(MgS)(001)/ nCaC(001)/3Cu(001)(semi-infinit) / - Fig.2.2a. The epitaxial relations are: CaC [100]||[100] LiCl(MgS); Cu [110]||CaC [100].

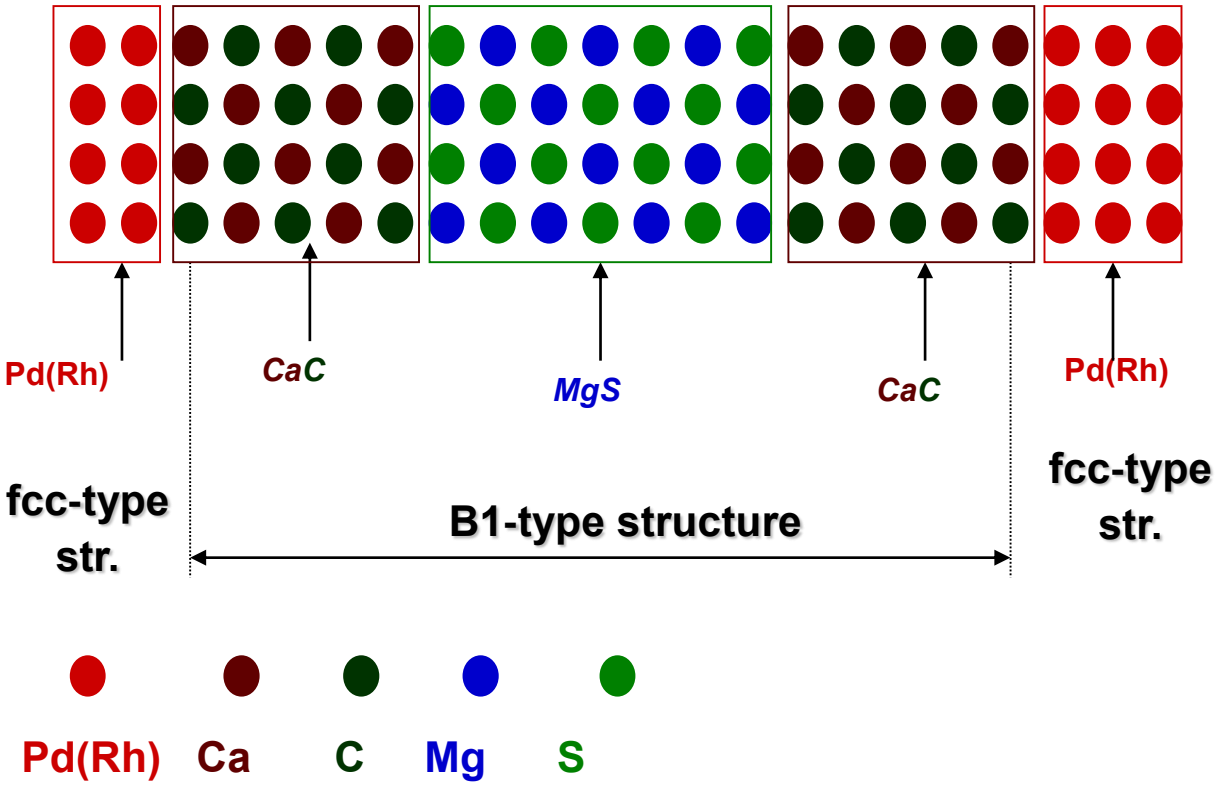


Fig.2.2a

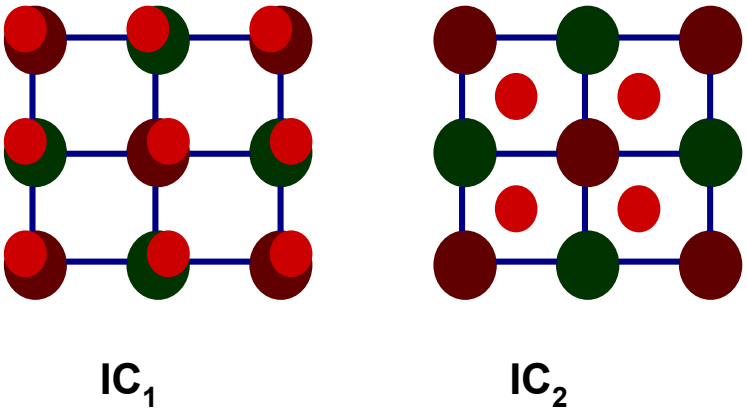


Fig.2.2b

The lattice parameters of heterojunction constituent materials are

$$a_{CaC} = a_{MgS};\ a_{CaC} = a_{Cu}\sqrt{2}$$

Two types of configurations were studied – Fig.2.2b:

IC_1 with Cu atoms sitting above Ca and C sites.

IC_2 with Cu atoms located above hollow sites between Ca and C.

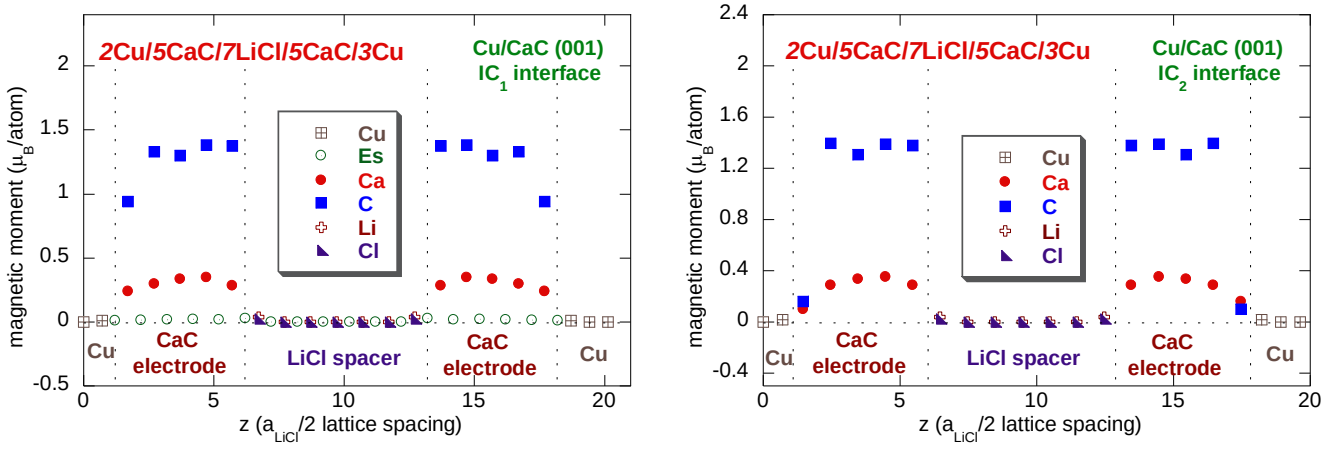


Fig.2.3a

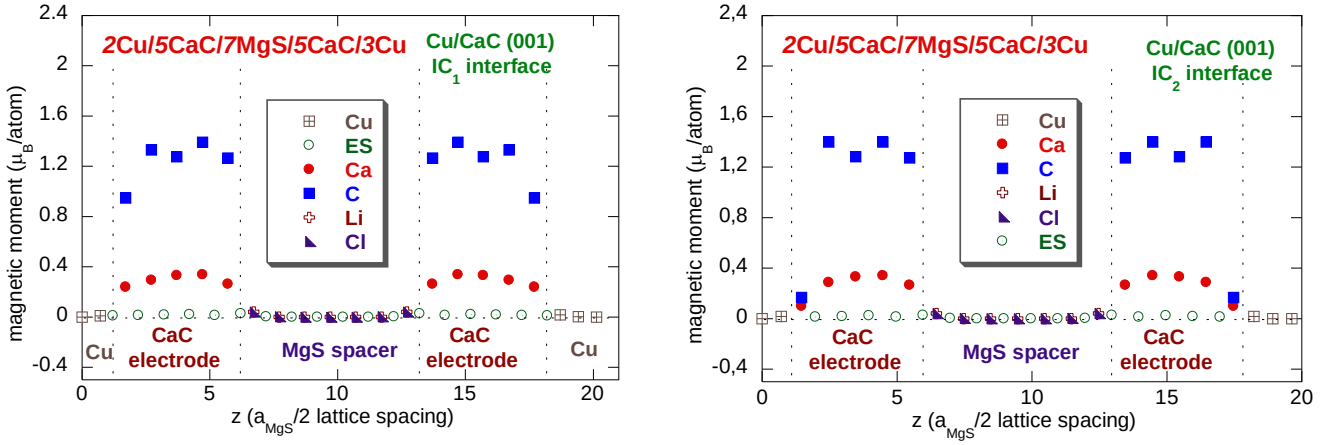


Fig.2.3b

The evolution of magnetic moments for the 2Cu/5CaC/7X/5CaC/3Cu(001) with X = LiCl and MgS, for both IC_1 and IC_2 configurations are given in Figs.2.3a and 2.3b. At larger distances from

interface, the CaC layers show a similar behavior as the bulk sample. The C and Ca magnetic moments at CaC/LiCl(MgS)(001) interfaces are little diminished as compared to values determined in bulk CaC sample. There are induced small polarizations on the interfacial Li(Mg) or Ca(S) sites.

The exchange couplings as function of barrier thickness, for the 2Cu/5CaC/mLiCl(MgS)/5CaC/3Cu(001) heterostructures, having IC_1 and IC_2 – type configurations are given in Fig.2.4. The exchange coupling are ferromagnetic, their amplitudes exponentially decreasing with barrier width.

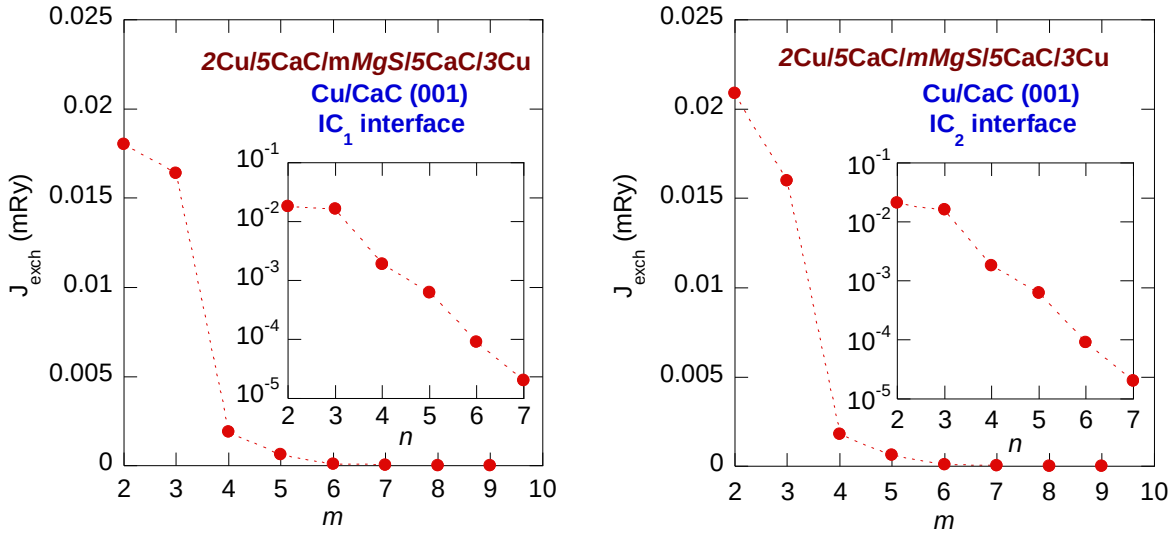


Fig.2.4

The spin-dependent transport properties were also analysed. The conductances depend on barrier type and decrease exponentially with the barrier thickness – Fig.2.5. In the ferromagnetic state, the main contributions to the conductivity are given by the minority spin electrons. There are predicted high values of the magnetoresistive ratio, of the 10^4-10^5, in case of 2Cu/5CaC/mLiCl/5CaC/3Cu heterostructures for m≥5.

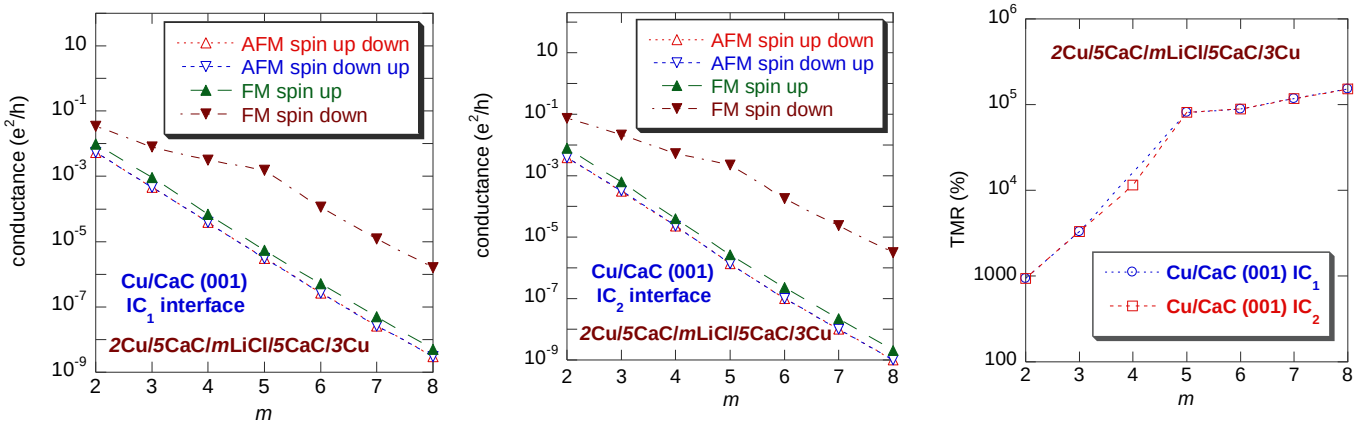


Fig.2.5

The $k_{||}$-resolved conductances of FM and AFM states for 2Cu/5CaC/5LiCl(MgS)/3Cu(001) magnetic tunneling junctions were studied. The results obtained in case of LiCl barrier are given in Fig.2.6. There are resonant states at CaS barrier. Thus, the resonant tunneling has a major role in spin polarized transport properties of the above junctions.

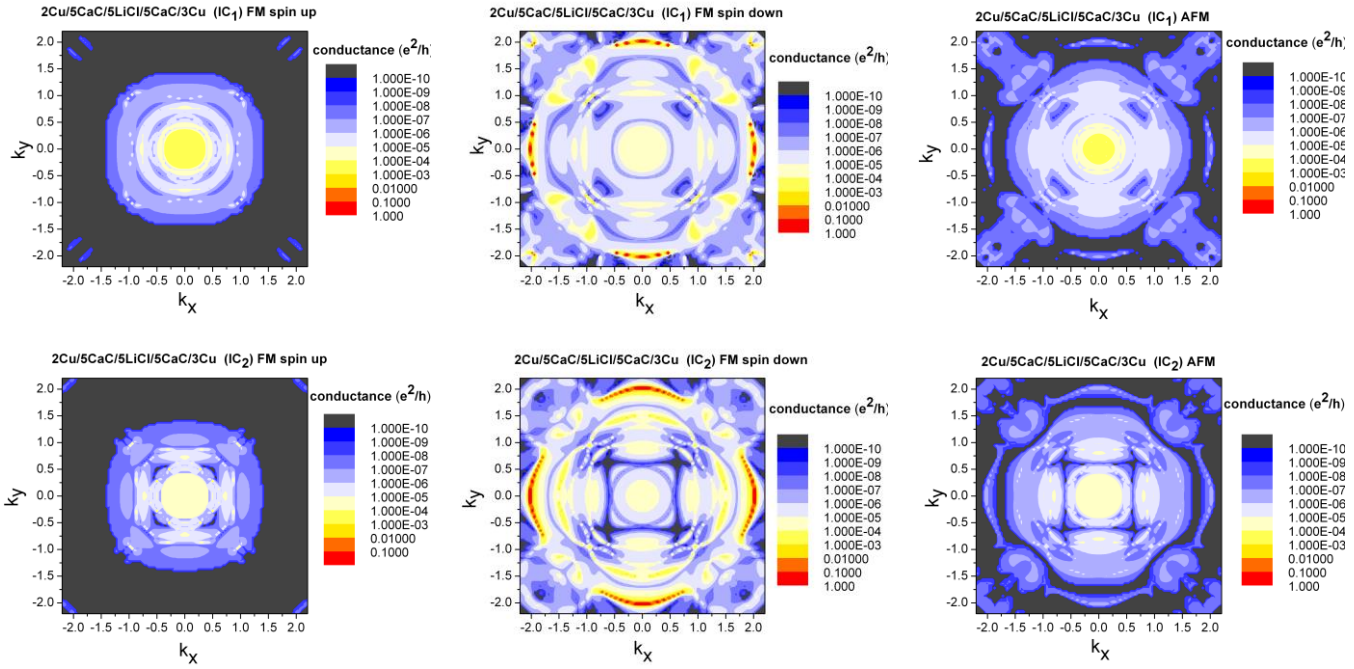


Fig.2.6

Some of the scientific results in the above heterostructures were presented at TIM14 Conference of Physics, Timisoara 20.11-22.11.2014

***„Electronic structure and spin polarized transport characteristics of CaC/LiCl(MgS)/CaC(001) heterojunctions”*, P.Vlaic, E.Burzo**

The paper will be published in AIP Conference Proceeding (ISI paper) in 2015.

3. (Ca,La,Fe,Mo)O_6-based double perovskites

The $Ca_{15}La_{0.5}FeMo_{1-x}W_xO_6$ perovskites with $x \leq 0.3$ were prepared by solid state reaction. The room temperature XRD patterns indicated the presence of the monoclinic type structure having space group $P2_1/n$. The degree of ordering, expressed by the percentage of atoms that are not misplaced, increased from ≅ 58 % (x = 0) to 77 % (x = 0.1) and 91 % (x = 0.3). In the above system the variable valence part of constituting ions can be described by $Fe_u^{3+}Fe_{1-u}^{2+}Mo_v^{5+}Mo_{1-v}^{6+}$. Starting from the determined compositions, according to charge neutrality rule, the relations between u and v parameters were determined: u = v+0.64 (x = 0), u = v+0.473 (x = 0.1) and u = v+0.384 (x = 0.3).

The neutron diffraction studies evidenced the presence of a ferrimagnetic type ordering. The magnetic moments at B and B’ sites are antiparallelly aligned. The magnetization isotherms, at 4 K, are in agreement with the above type of magnetic ordering – Fig.3.1. The saturation magnetizations increase significantly as the W content is higher. The temperature dependences of the magnetizations in ZFC and FC, in a field H = 1 kOe, evidences moderate irreversibilities at temperatures T < 200 K, suggesting a

cluster glass contribution to the magnetization – Fig.3.2. This is superposed on an essential ferrimagnetic type ordering.

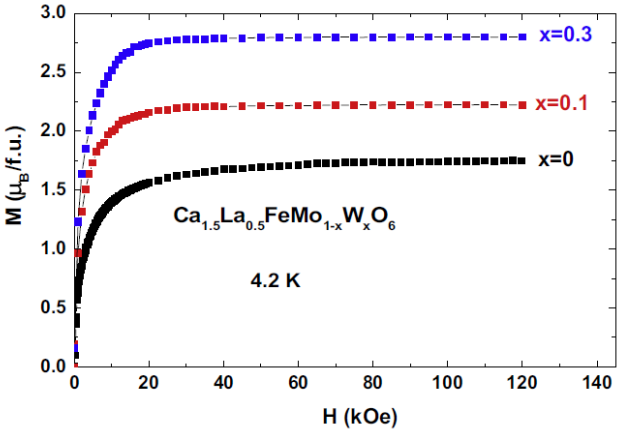


Fig.3.1

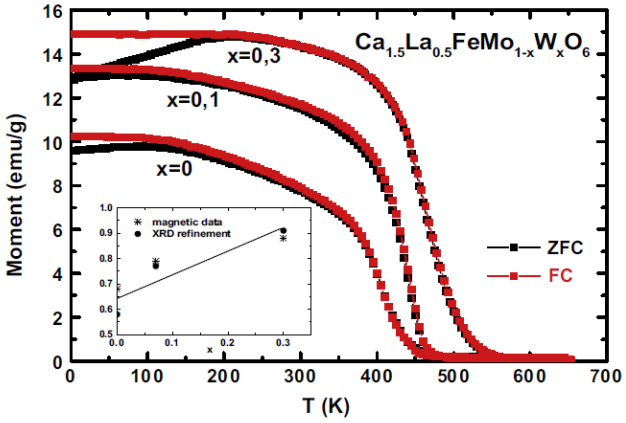


Fig.3.2

The temperature dependences of the magnetic susceptibilities can be described by a Néel-type relation, characteristic for ferrimagnetic ordering – Fig.3.3.

$$\chi^{-1}=\chi_0^{-1}+TC^{-1}-\sigma(T-\theta) \qquad (1)$$

by C is denoted the Curie constant and the χ_0, σ and θ parameters are determined by the molecular field coefficients describing by the exchange interactions between and inside the magnetic sublattices.

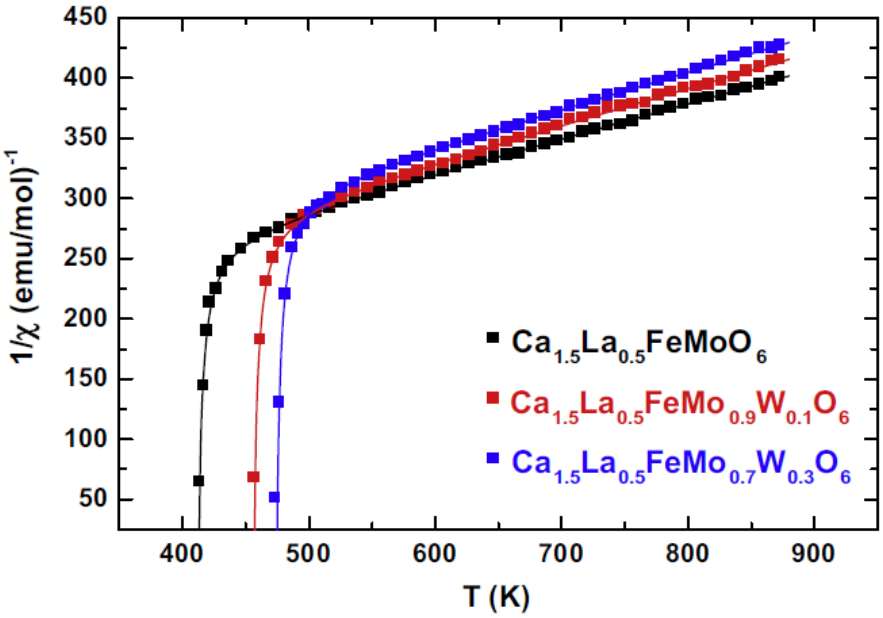


Fig.3.3

The Curie constants decrease as the Mo is gradually substituted by W. This behavior can be attributed to changes in valence states of some iron and molybdenum ions. Admitting that their Curie constants, $C_{Fe^{2+}}$, $C_{Fe^{3+}}$ and $C_{Mo^{5+}}$, are given by those of free ions values, a second relation connecting the u and v parameters has been obtained

$$C = uC_{Fe^{3+}} + (1-u)C_{Fe^{2+}} + vC_{Mo^{5+}} \qquad (2)$$

In this way the evolution with composition of the number of magnetic ions in the two valence states has been obtained. Thus, in $Ca_{1.5}Fe_{0.5}MoO_6$ perovskite there are $0.70Fe^{2+}$ and $0.68Mo^{5+}$ ions per formula unit. When increasing the tungsten content from x = 0 to x = 0.3, the number of Fe^{2+} ions increases by 10 % and those of Mo^{5+} decreased by 19 %.

Assuming a two sublattices molecular field model, the mean exchange interactions between and inside the B and B' magnetic sublattices were determined.

The temperature dependences of the resistivities, ρ, are plotted in Fig.3.4. The resistivities decrease up to temperatures 204 K- 249 K (depending on composition), where a change in slope, due to semiconducting-metal transition is observed. The resistivities, at T = 10 K, increase as the tungsten content is higher. The above perovskites can be viewed, due to presence of $W^{6+}(Mo^{6+})$ ions, as a distribution of metallic and insulating domains. The increase of the (W^{6+}, Mo^{6+}) content rises the proportion of insulating regions with respect to the metallic region and make the system more and more semiconducting. For the sample with x = 0.3, the resistivities in the temperature range 18 K ≤ T ≤ 160 K follow a nearly linear temperature dependence on $T^{-1/4}$, as predicted by the VRH process.

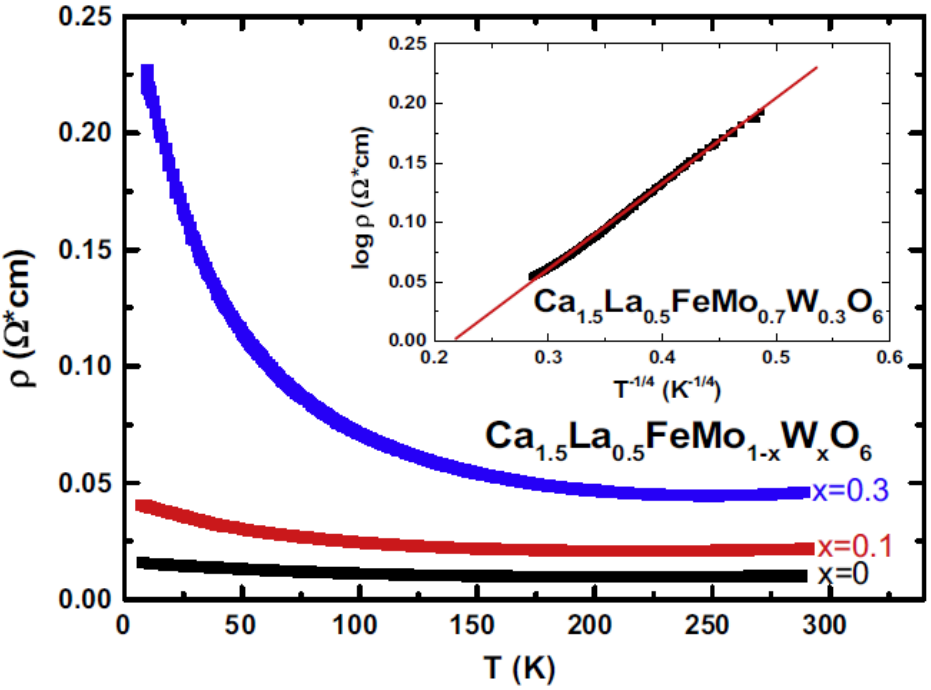


Fig.3.4

The temperature and field dependences of the magnetoresistivities were also studied. Some data are plotted in Fig.3.5. The experimental data were analysed considering the presence of a spin tunneling mechanism between grains at low fields and intragrain contributions in high internal fields. The model describes correctly the experimental data, as can be seen in Fig.3.5.

The spin polarizations, P, at 10 K, increases from 0.40 (x = 0) to 0.50 (x = 0.3). The spin polarizations decrease linearly with temperature with near the same rate, of $1 \cdot 10^{-3}$ K^{-1}, for all the studied compositions. The extrapolation at P= 0, gives temperatures near the same as their Curie points – Fig.3.6.

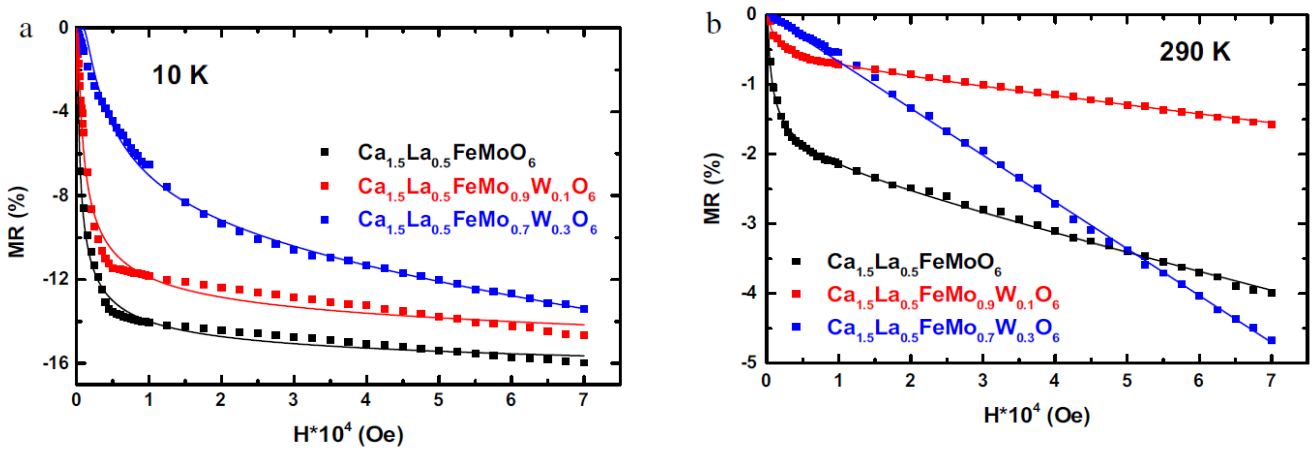


Fig.3.5

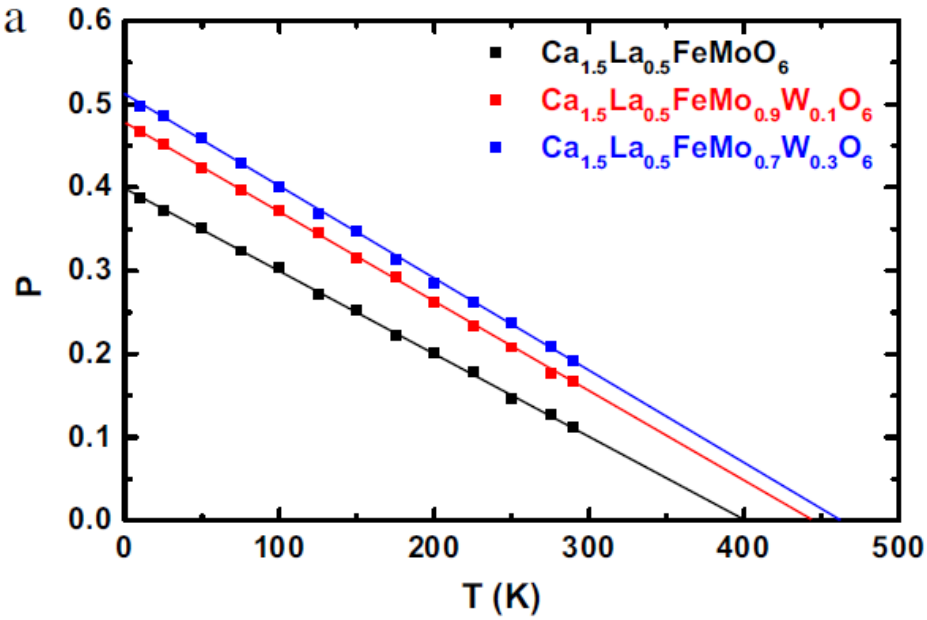


Fig.3.6

The above system of perovskites were included in the research program for 2015 year. Since some studies were performed in the second part of 2014 year, the scientific results were rapidly accepted for publication, and included in the following paper.

1. "***Magnetic and transport properties of $Ca_{1.5}La_{0.5}FeMo_{1-x}W_xO_6$ perovskites***,,, **E.Burzo, I.Balasz,** M.Valeanu, D.P.Kozlenko, S.E.Kichanov, A.V.Rutkaukas, B.N.Savenko Journal of Alloys and Compounds 621, 71 (2015), IF = 2.734

2. "***Magnetoresistive properties of $La_{1.5}Ca_{0.5}FeMo_{1-x}W_xO_6$ double perovskites***,,, **E.Burzo, I.Balasz,** M.Valeanu and D.P.Kozlenko

7th International Conference on Material Science and Condensed Matter Physics, Chișinău, 16.09-19.09.2014, Paper ABM 11B, p.104. INIS indexed.

4. Magnetic properties of rare-earth-cobalt (iron) intermetallic compounds

The rare-earth (R)-transition metal M (M = Fe, Co) compounds have interesting properties with technical applications, as high crystalline anisotropy, magnetostriction or magnetoresistance. As a result the magnetic properties of these systems, particularly the magnetic-non magnetic transition as effect of pressure or determined by external or exchange fields are studied.

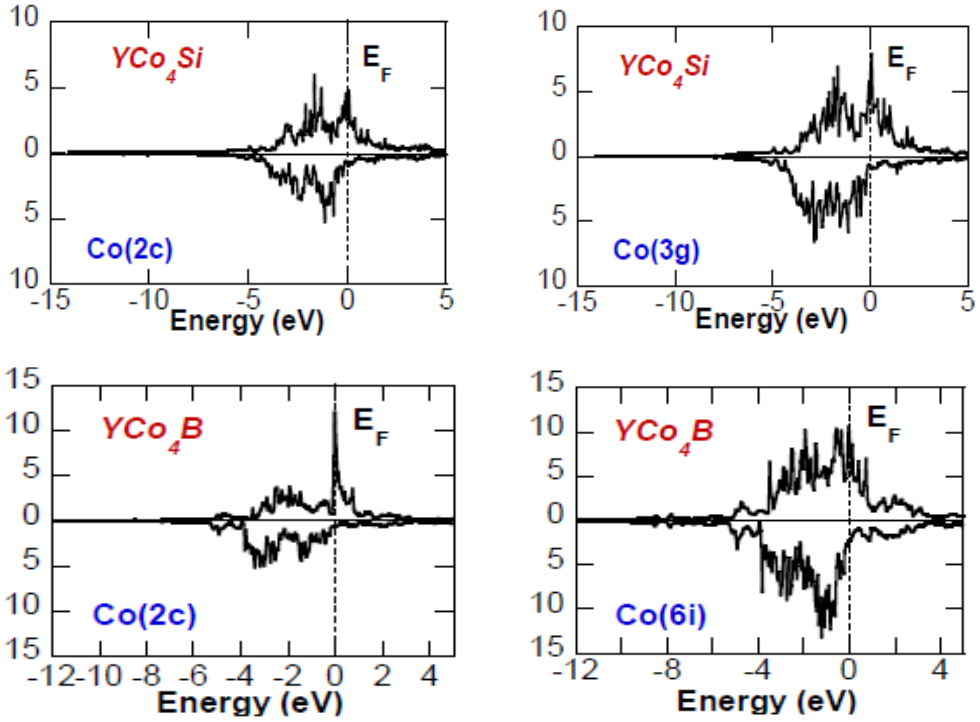


Fig.4.1

As example in Fig.4.1, the partial and total densities of states of Co2c and Co3g atoms in YCo_4Si and Co2c and Co6i in YCo_4B, at normal conditions, are shown. The partial substitution of Co by Si leads to a significant decrease of Co2c magnetic moment, as compared to the value determined in end series compound, YCo_5. As effect of pressure, relative volumes (v/v_0) decrease respectively, there is a linear variation of cobalt moments, as both sites, with the same slope. For a relative volume $v/v_0 = 0.92$, there is a magnetic transition from the high spin state (HS) to low spin state (LS) – Fig.4.2. The pressure response of cobalt moments at 2c and 6i sites in YCo_4B is somewhat different – Fig.4.3. For a reduced volume $v/v_0 = 0.90$, the cobalt moment at 6i site vanishes, while that at Co2c site decreases up to $M_{Co} = 0.16\ \mu_B$ and is nil only for a relative volume $v/v_0 = 0.85$. The theoretical pressure studies on $Y_3Co_{11}B_4$ or $Y_2Co_7B_3$, where the cobalt moments are rather low, evidenced their direct collapse at critical v/v_0 value. Thus, as function of the cobalt moments, the magnetic-non-magnetic transition can involve either one step or two steps dependences.

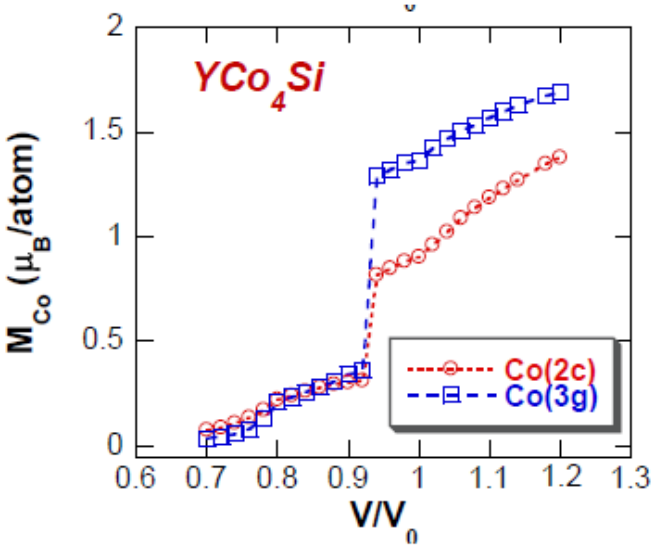


Fig.4.2

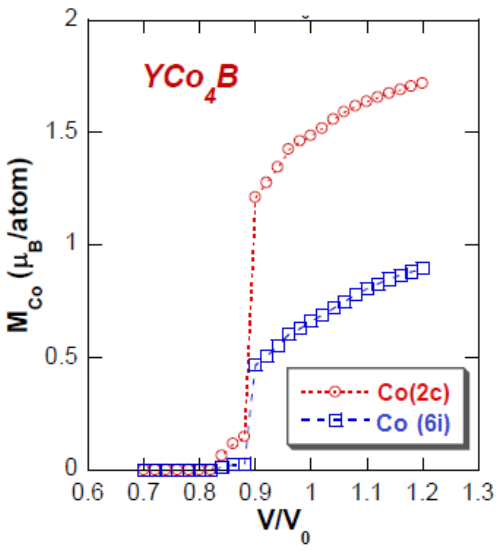


Fig.4.3

The study of magneto-volume effect in R-Co or R-Fe can give interesting information on the degree of localization of transition metal moments. The volume effect can be analysed as function Γ parameter, $\Gamma = d\ln T_c/d\ln v$. In the case of localized moment, the Γ dependence on the Curie temperatures can be described by the relation:

$$\Gamma = a - bT_c \qquad (1)$$

while in case of an itinerant model has de form:

$$\Gamma = A + BT_c^{-2} \qquad (2)$$

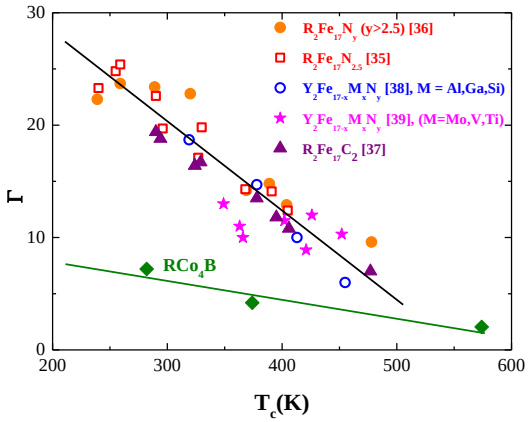


Fig.4.4

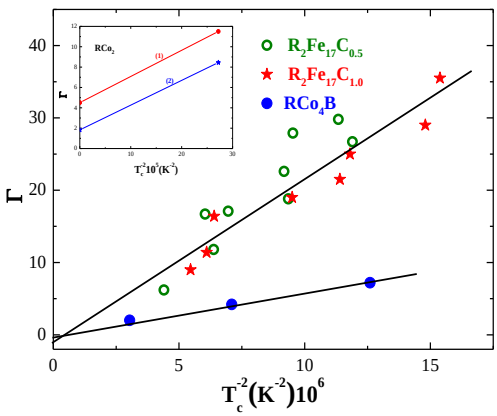


Fig.4.5

Both above type dependences can be evidenced in R-Fe and R-Co compounds – Fig.4.4 and 4.5. In the studied systems there is a correlation between sample volumes and T_c values, although the involved mechanisms are different in R-Fe and R-Co compounds, respectively. Thus, in $R_2Fe_{17}C(H)_y$ the Fe atoms are distributed in four types of lattice sites, the distances between iron atoms being different. The exchange interactions involving iron atoms located at distances d ≤ 2.45 Å are negative, while those

associated with iron atoms situated at longer distances are positive. Since the positive exchange interactions dominate, the negative ones are not satisfied. As a result the Curie temperatures decrease. When volumes increase, as result of the presence of interstitial atoms, the intensities of negative exchange interactions decrease and finally cancel. As a result, the Curie temperatures increase. Since there is an increase of volumes, the Fe3d bands narrow and their degree of iron moment localization is increased. Thus, when the number of interstitial atoms increase as well as the volume, the $\Gamma = f(T_c)$ relation change from a T_c^{-2} dependence to T_c one, from itinerant to more localized moment, respectively.

The cobalt magnetic moments, unlike those or iron, are strongly affected by pressure. These decrease when the pressure increases, relative volumes diminish, respectively. The exchange interactions decrease in a similar way as the Curie temperatures. Thus in R-Co compounds, the volume effects can be mainly correlated with the changes of the cobalt moments, parallelly with those of T_c values.

The non-magnetic to magnetic transitions in R-Co compounds were also studied. At a critical exchange or external field, for an exchange enhanced paramagnet, there is a sudden change to a magnetic state as result of the exchange splitting of their 3d band. At higher external field than the critical one, there is a linear dependence of cobalt (nickel) moments on exchange fields. The exchange splitting of 3d band is well correlated with their moments as illustrated in case of RNi_4B compounds – Fig.4.6. The above behavior can be described in induced magnetism model.

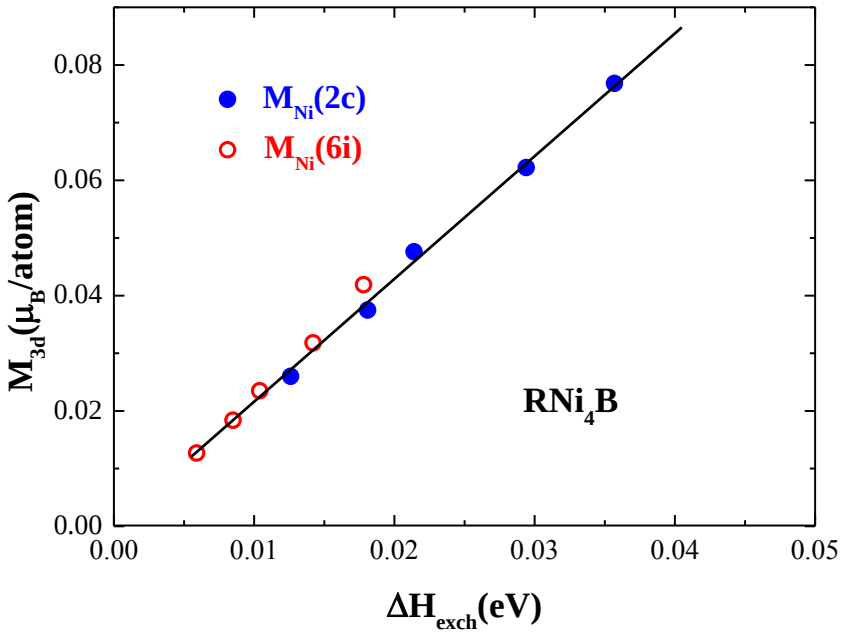


Fig.4.6

The exchange interactions between R and M atoms in R-M compounds have been analysed in 4f-5d-3d model, taking place through the R5d band polarizations. The R5d band polarizations are determined both by 4f-5d local exchange as well as by 5d-3d short range interactions. The R5d band has a great extension, of 5.33 Å, respectively. As function of temperature, the distances between R and M

atoms are little modified, comparatively with extension of R5d band. Thus, there are present 5d-3d exchange interactions even in exchange enhanced paramagnet as $LuCo_2$ (T = 100 K), as evidenced in the presence of external field. In a field of H = 57.2 kOe, a cobalt moment of 0.016 μ_B is evidenced, parallelly with a Lu5d band negative polarized, of -0.007 μ_B. The same behavior can be seen in RCo_2 compounds at $T > T_c$. The above scientific results on rare-earth-transition metal compounds were presented, as invited lectures, at the following international conferences:

1. ***Pressure effects on the magnetic behavior of cobalt in rare-earth compounds***

   E.Burzo, P.Vlaic, D.P.Kozlenko

   Balkan Workshop on Applied Physics, 4.06-6.06. 2014 Constanta (Invited lecture). Romanian Journal of Physics 60, 1-2 (2015). IF = 0.75

2. Magnetic properties and electronic structures of rare-earth transition metal compounds

   E.Burzo

   7th International Conference on Material Science and Condensed Matter Physics, 16.09-19.09. 2014 Chișinău (Invited lecture). Indexed INIS.

3. Exchange enhanced parramagnetism of rare-earth(yttrium)-transition metal compounds

   E.Burzo

   TIM14 Physics Conference, 20.11-22.11.2014, Timisoara (Invited lecture).

   AIP Conf. Proc. (2015).

The scientific results, during 02.09.2013-31.12.2014 period were published, accepted for publication or presented at international conferences as below indicated:

1. ***Structural, electronic, magnetic and spin dependent transport properties of Fe/CaS/Fe(001) heterostructures"***

   P. Vlaic, E.Burzo, K. Carva,

   J. Appl.Phys. 113, 053715 (2013) IF = 2.185

2. ***Pressure effects on crystal structures and magnetic properties of RCo_5 (R = Y or Gd) compounds***

   E.Burzo, P. Vlaic,

   AIP Conf. Proc. 1564, 96 (2013) ISI journal

3. ***Impact of Fe/NaCl(001) interface structure on electronic, magnetic and spin polarized transport of Fe/NaCl/Fe(001) heterojunctions: An-ab initio study***

   P.Vlaic, E.Burzo, K.Carva

   J. Alloys Comp. 598, 41 (2014) IF = 2.734

4. ***Magnetic and transport properties of $Ca_{1.5}La_{0,5}FeMo_{1-x}W_xO_6$ perovskites***

   E.Burzo, I.Balasz, M.Valeanu, D.P.Kozlenko, S.E.Kichanov, A.V.Rutkaukas, B.N.Savenko

   J.Alloys. Comp. 621, 71 (2015) IF = 2.734

5. ***Oscillatory exchange coupling and strong direct tunneling in AgCl based heterojunctions***

P.Vlaic, E.Burzo, K.Carva

J.Alloys Comp. (accepted for publication)

6. ***Pressure effects on the magnetic behaviour of cobalt in rare-earth compounds***

   E.Burzo, P.Vlaic, D.P.Kozlenko

   Rom. J.Phys. 60, 1-2 (2015) IF = 0.745

7. ***Magnetic and spin dependent transport properties of SrC/NaCl/(CaS)/SrC (001) tunnel junctions***

   P. Vlaic, E. Burzo

   "Fifth Seeheim Conference on Magnetism" Frankfurt, Germany, 29.09 –3.10.2013

8. ***Electronic structure and spin polarized transport characteristics of CaC/LiCl(MgS)/CaC(001) heterojunctions***

   P.Vlaic, E.Burzo

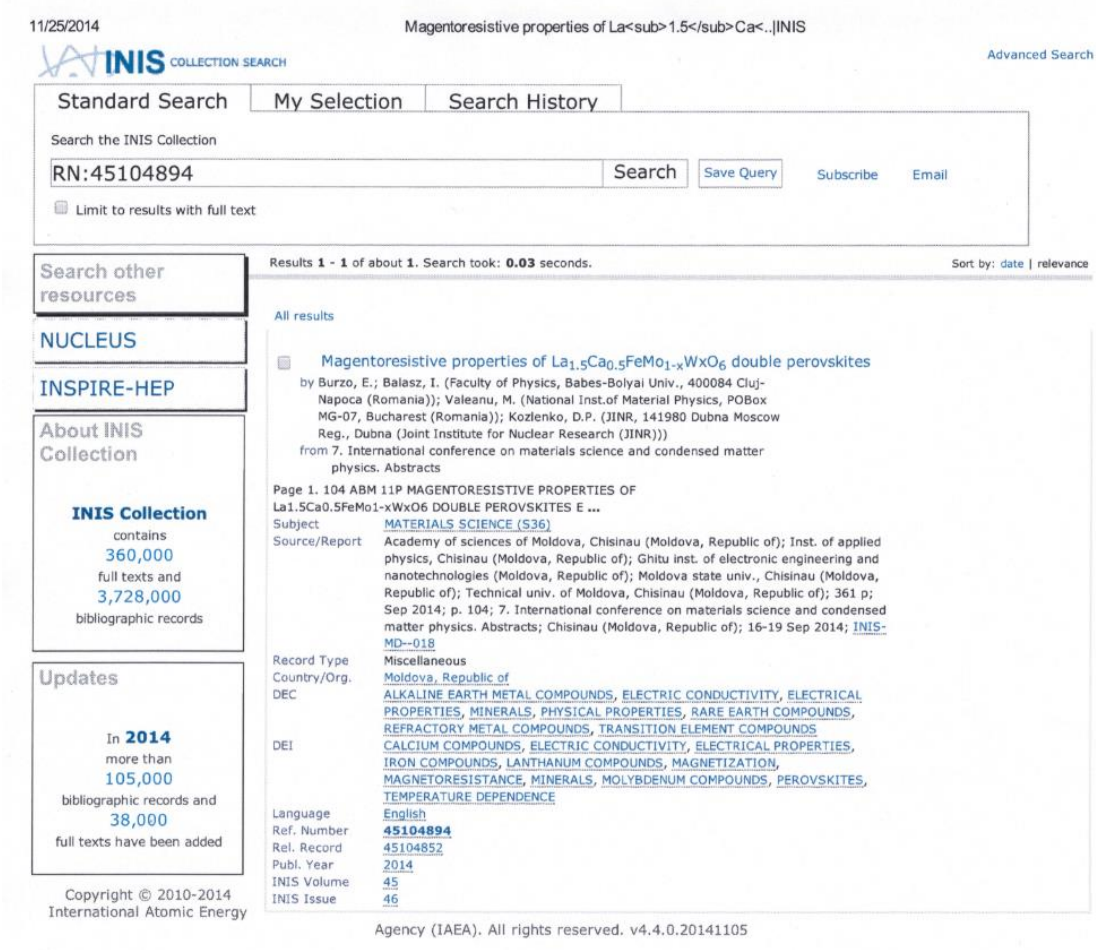
   TIM-14 Phys. Conference, 20.11-22.11.2014 (Oral presentation), will appear in AIP Conf. Proc., 2015 (ISI paper).

9. ***Magnetoresistive properties of $La_{1.5}Ca_{0.5}FeMo_{1-x}W_xO_6$ double perovskites***

   E.Burzo, I.Balasz, M.Valeanu, D.P.Kozlenko

   7th International Conference on Material Science and Condensed Matter Physics, Chișinău, paper ABM 11B p.104 (Poster presentation)

   INIS indexed

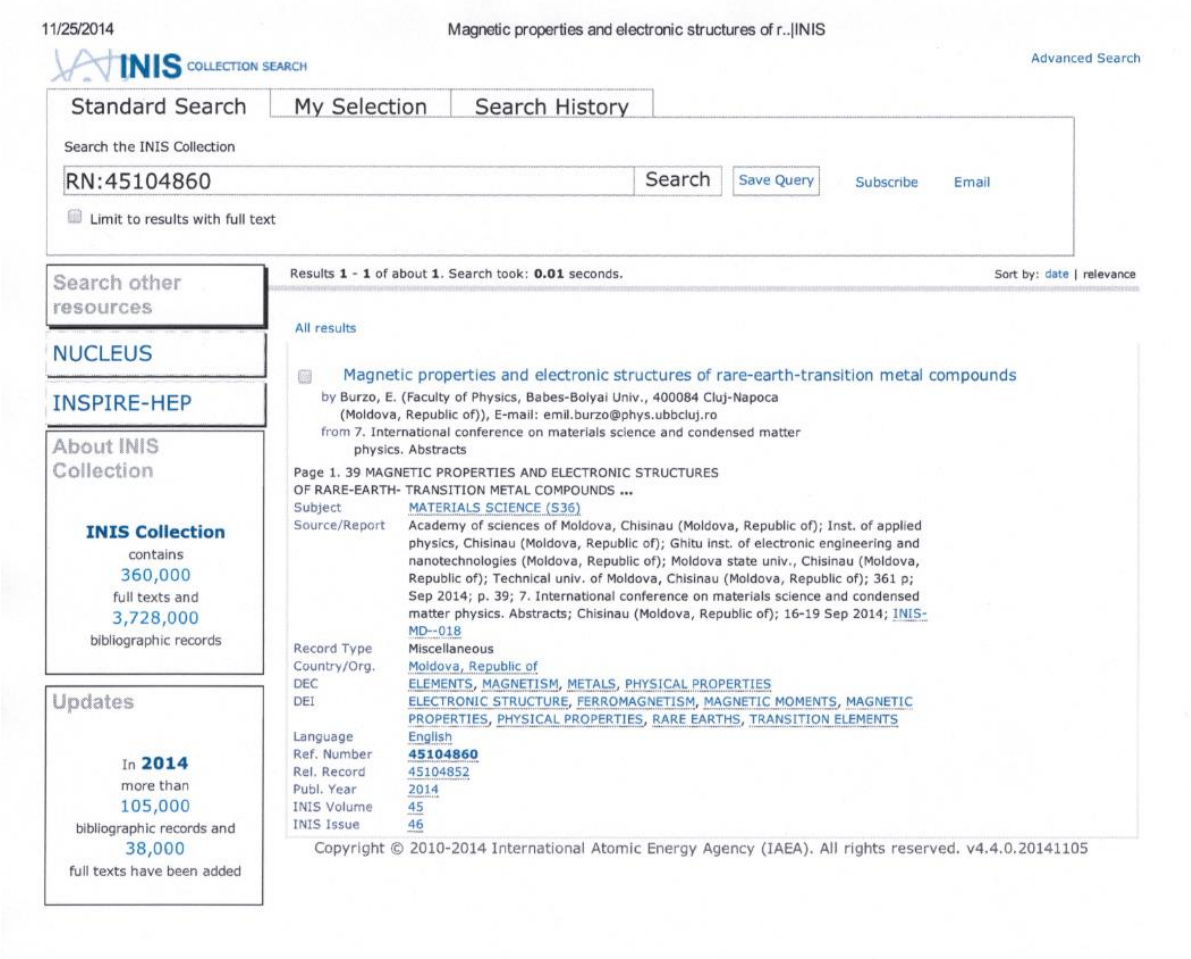


10. ***Magnetic properties and electronic structures of rare-earth transition metal compounds***

E.Burzo

Invited lecture at the 7th International Conference on Material Science and Condensed Matter Physics, Chișinău, p.39.

INIS indexed



11. ***Exchange enhanced paramag netism of rare-earth (yttrium)- transition metal compounds***

E.Burzo

TIM-14 Phys. Conference, 20.11-22.11.2014 (Invited lecture), will be published in AIP Conf. Proc., 2015 (ISI paper).

*

* *

The papers, even recently published were cited in scientific journals and that published in J. Appl. Phys. 113, 053715 (2013) has been considered as "hot paper".

Project Manager,

Acad. Prof. dr. Emil Burzo